 Bull. Chem. Soc. Jpn., 76, 2307–2313 (2003)

Assemblies Possessing Rich Hydrogen Bonds Derived from *trans*-Oxamidato-Bridged Dicopper(Ⅱ) Complexes and Carboxyl Auxiliary Ligands

Hua-Xin Zhang,*,# Bei-Sheng Kang,*,# Zhong-Ning Chen, Cheng-Yong Su, and Kai-Bei Yu†

School of Chemistry and Chemical Engineering, Zhongshan University, Guangzhou, Guangdong 510275, China

†Chengdu Institute of Organic Chemistry, Chinese Academy of Sciences, Chengdu, Sichuan 610041, China

Received April 7, 2003; E-mail: ceszhx@zsu.edu.cn

Three complexes $[\{Cu_2(trans\text{-oxap})(nic)(H_2O)_2\}_n](ClO_4)_n \cdot 0.5nH_2O$ **1**, $[Cu_2(trans\text{-oxen})(nic)_2(H_2O)_2] \cdot 2H_2O$ **2**, $[Cu_2(trans\text{-oxen})(hyba)_2(H_2O)_2]$ **3** have been obtained from reactions of the *trans*-oxamidato-bridged dicopper(Ⅱ) unit $[Cu_2(trans\text{-L})]^{2+}$ (L = oxen or oxap, H_2oxen = *N*,*N*′-bis(2-aminoethyl)oxamide, H_2oxap = *N*,*N*′-bis(2-aminopropyl)oxamide) with the auxiliary ligands hydroxybenzoic acid (Hhyba) and nicotinic acid (Hnic). Their structures were determined by X-ray crystallography. Results showed that polymeric chains are formed in **1**, since the auxiliary ligand nic behaves as the spacer connecting the dicopper units. However, **2** and **3** contain only discrete dinuclear units, since nic in **2** and hyba in **3** are terminal ligands. Chains in **1** and dinuclear units in **2** and **3** further fabricate extended structures through hydrogen bonds. The structural diversity of these complexes results from the different affinity of the coordination donors to the copper(Ⅱ). The magnetic property is exemplified by **3**; thermal behaviors of all complexes have been investigated.

Interest in supramolecular chemistry has increased at a tremendous rate during the last two decades since this interdisciplinary field blurs most of the traditional divisional boundaries of science and mixes chemistry, biology and material science.[1] Simultaneously, metallosupramolecules have become the subject of many recent studies.[2] The employment of metal centers and coordination chemistry for directing the formation of complex structures has evolved into one of the most widely used strategies for organizing molecular building blocks into supramolecular architectures, with coordination polymers being the representatives.[3] In the pursuit of supramolecular structures with desired functions and fascinating topologies, more and more attention has been paid to the combinational utilization of metal–ligand interactions and intermolecular interactions, such as hydrogen bonding, electrostatic force, charge transfer, and π–π stacking, during the assembly process of extended networks,[4] since the result of the balance and competition between these interactions is important and may affect the bulk properties of the resulting complexes. Though progress in this respect has been achieved, our mastery of these subtle interactions as synthetic tools is still in an early stage of development.

We have been interested in metallosupramolecular systems assembled from *trans*-oxamidato-bridged dicopper(Ⅱ) units.[5–7] The *N*,*N*′-disubstituted oxamides are bis-tridentate ligands when adopting the *trans*-conformation; they favor the formation of dicopper(Ⅱ) units (Scheme 1), which are excellent building blocks for supramolecular networks.[5–9] Extended systems with one-, two- or three-dimensionality can be obtained by assembling these binuclear units with multi-connecting ligands (called spacers). In the dicopper unit, three of the coordination sites of each copper atom have been occupied by the atoms (N, N, O) of the oxamide. Considering the coordination geometry of the copper ion, one sees that the remaining coordination sites of a copper atom are directional (one equatorial position and two axial positions). Our previous work on the assembly of these building blocks with a variety of spacers has shown that the structural topology of the resulting complexes depends on a number of factors including the orientation of the coordinating donor in the spacers, the flexibility of the spacers, the coordination modes, and reaction conditions. One- and two-dimensional structures are readily obtained through metal–ligand interactions, whereas 3-D networks are usually constructed by 1- or 2-D polymeric parts through hydrogen bonding interactions.[6–8] To further investigate the assembly mechanism of the *trans*-oxamidato-bridged dicopper units with various auxiliary ligands, we have selected car-

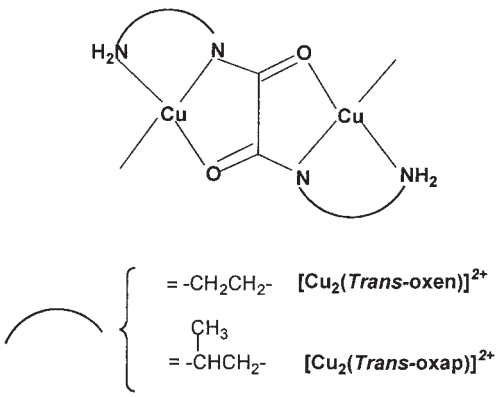

Scheme 1.

State Key Laboratory of Rare Earth Materials Chemistry and Applications, Peking University, Beijing, China

Published on the web December 15, 2003; DOI 10.1246/bcsj.76.2307

boxylic acids nicotinic acid (Hnic) or 4-hydroxybenzoic acid (Hhyba), which possess two different functional groups, to react with the dicopper units and we have studied the effect of acidity on the structures.

Experimental

Materials. All chemicals, unless otherwise indicated, were purchased from commercial sources and used as received. [Cu(oxen)]·$2H_2O$ and [Cu(oxap)] were synthesized according to the methods in references.[17] **Caution!** Though no danger was encountered in this work, perchlorate salts containing organic ligands are potentially explosive. They should be prepared in small qualities and handled with care.

[{Cu_2(*trans*-oxap)(nic)(H_2O)}$_n$](ClO_4)$_n$·0.5*n*H_2O 1: To an aqueous solution (40 cm^3) of Cu(oxap) (0.264 g, 1.0 mmol) was added $Cu(ClO_4)_2$·$6H_2O$ (0.371 g, 1.0 mmol) while stirring, followed by the addition of an aqueous solution (10 cm^3) containing nicotinic acid (0.123 g, 1.0 mmol) and an equivalent amount of NaOH (0.040 g, 1.0 mmol). After being stirred for several minutes, the mixture was filtered; the filtrate was allowed to stand at room temperature for a week to yield blue-black crystals. Yield: ~43%. Anal. Calcd for $C_{28}H_{50}Cu_4Cl_2N_{10}O_{21}$: C, 28.31; H, 4.24; N, 11.79%. Found: C, 28.29; H, 4.13; N, 11.78%. IR (KBr, cm^{-1}): 1581 $\nu_{as}(COO^-)$, 1356 $\nu_s(COO^-)$, 1103, 620 (ClO_4^-).

[Cu_2(*trans*-oxen)(nic)$_2$(H_2O)$_2$]·$2H_2O$ 2: To an aqueous solution (40 cm^3) of Cu(oxen) (0.272 g, 1.0 mmol) was added $Cu(ClO_4)_2$·$6H_2O$ (0.371 g, 1.0 mmol) while stirring, followed by the addition of an aqueous solution (10 cm^3) containing nicotinic acid (0.246 g, 2.0 mmol) and equivalent NaOH (0.08 g, 2.0 mmol). After being stirred for several minutes, the mixture was filtered and the filtrate was allowed to stand at room temperature for a week to yield blue-black crystals. Yield: about 78%. Anal. Calcd for $C_{18}H_{28}Cu_2N_6O_{10}$: C, 35.12; H, 4.58; N, 13.65%. Found: C, 34.78; H, 4.51; N, 13.52%. IR (KBr pellets, cm^{-1}): 1588 $\nu_{as}(COO^-)$, 1356 $\nu_s(COO^-)$.

[Cu_2(*trans*-oxen)(hyba)$_2$(H_2O)$_2$]$_n$ 3: To an aqueous solution (40 cm^3) of Cu(oxen)·$2H_2O$ (0.272 g, 1.0 mmol) was added $Cu(ClO_4)_2$·$6H_2O$ (0.371 g, 1.0 mmol), the reddish-violet color turned blue while stirring. An aqueous solution (10 cm^3) of 4-hydroxybenzoic acid (0.138 g, 1.0 mmol) and equivalent sodium hydroxide (0.04 g, 1.0 mmol) was then added. After being stirred for several minutes, the mixture was filtered and the filtrate was allowed to stand at room temperature for a week to yield blue-black crystals. Yield: ~40%. Anal. Calcd for $C_{20}H_{26}Cu_2N_4O_{10}$: C, 39.41; H, 4.30; N, 9.19%. Found: C, 39.22; H, 4.27; N, 9.28%. IR (KBr pellets, cm^{-1}): 1581 $\nu_{as}(COO^-)$, 1384 $\nu_s(COO^-)$.

Physical Measurements. IR spectra were recorded on a Nicolet FT-IR-170SX spectrophotometer as KBr pellets in the 4000–400 cm^{-1} region. The TG analyses were carried on a Perkin-Elmer TGA7 system under the nitrogen atmosphere. Variable-temperature magnetic susceptibilities in the temperature range 2–300 K were measured on a CF-1 extracting-sample magnetometer at a magnetic field of 5.0 T with the powdered samples kept in capsules for weighing. Diamagnetic corrections were estimated from Pascal tables.

X-ray Crystallography. Single crystals with suitable dimensions were mounted on glass fibers and data collections were performed on a Siemens P4 diffractometer for **1** and **3** by ω scan, and on a Bruker CCD Area Detector Diffractometer for **2** by φ and ω scans using the graphite-monochromated Mo-Kα radiation ($\lambda = 0.71073$ Å). For all complexes, the coordinates of the metal atoms were determined by direct methods; then the remaining non-hydrogen atoms were located from successive difference Fourier syntheses. The structures were refined by full-matrix least-squares techniques with anisotropic thermal parameters for all the non-hydrogen atoms.

All hydrogen atoms of **1** were located on the ΔF map. The hydrogen atoms of **2** were located on the ΔF map, while those of C(5) were added theoretically. The hydrogen atoms of **3** were added theoretically, while those of water molecules were located on the ΔF map. The oxygen atoms of ClO_4^- in **1** are disordered; with the occupancy factor of 0.5 at each position. The calculations for **1** and **3** were performed with the Siemens SHELXL/PC program package.[18] The calculations for **2** were performed with the Bruker SHELXL/PC program package.[19] A summary of their crystallographic data is given in Table 1. The selected atomic distances and bond angles are presented in Tables 2, 3, and 4, for **1**, **2**,

Table 1. Crystallographic Data for **1**, **2**, and **3**

Complexes	**1**	**2**	**3**
Formula	$C_{14}H_{25}N_5O_{10.50}Cu_2Cl$	$C_{18}H_{28}N_6Cu_2O_{10}$	$C_{20}H_{26}Cu_2N_4O_{10}$
fw	593.92	615.54	609.53
Space group	$P\bar{1}$	$P2_1/c$	$P2_1/n$
a/Å	7.3710(9)	19.142(3)	13.4890(10)
b/Å	12.710(2)	9.2423(13)	9.0900(10)
c/Å	13.204(2)	13.3498(18)	19.4680(10)
α/deg	111.97(3)		
β/deg	97.088(3)	97.184(3)	106.460(10)
γ/deg	97.937(3)		
V/Å^3	1120.3(2)	2343.3(6)	2289.2(3)
Z	2	4	4
ρ_{calcd}/g m^{-3}	1.761	1.745	1.769
μ/cm^{-1}	20.81	18.82	19.24
T/°C	20(2)	20(2)	17(2)
R[a)]	0.0450	0.0340	0.0264
wR[b)]	0.1077	0.0788	0.0620

1: $w = [\sigma^2(F_o^2) + (0.07090P)^2]^{-1}$. $P = (F_o^2 + 2F_c^2)/3$.
2: $w = [\sigma^2(F_o^2) + (0.0464P)^2]^{-1}$. $P = (F_o^2 + 2F_c^2)/3$.
3: $w = [\sigma^2(F_o^2) + (0.0385P)^2]^{-1}$. $P = (F_o^2 + 2F_c^2)/3$.

Table 2. Selected Bond Distance (Å) and Angles (°) for **1**

Cu1–N1	1.913(2)	Cu1–N5	1.975(2)
Cu1–O1	2.0112(13)	Cu1–N2	2.062(2)
Cu2–N3	1.9239(14)	Cu2–O3	1.9326(12)
Cu2–N4	2.010(2)	Cu2–O2	2.024(2)
Cu2–O2w	2.351(2)	Cu1···Cu1a[a)]	5.227
Cu2···Cu2a[b)]	5.296		
N1–Cu1–N5	174.01(6)	N1–Cu1–O1	83.76(6)
N5–Cu1–O1	93.88(6)	N1–Cu1–N2	81.75(7)
N5–Cu1–N2	100.50(7)	O1–Cu1–N2	165.49(6)
N3–Cu2–O3	162.77(6)	N3–Cu2–N4	82.60(7)
O3–Cu2–N4	101.63(6)	N3–Cu2–O2	82.58(6)
O3–Cu2–O2	92.31(6)	N4–Cu2–O2	165.16(6)
N3–Cu2–O2w	106.90(6)	O3–Cu2–O2w	90.01(5)
N4–Cu2–O2w	88.20(7)	O2–Cu2–O2w	96.93(6)

Symmetry codes: a) $2-x$, $1-y$, $2-z$. b) $-1-x$, $1-y$, $1-z$.

Table 4. Selected Bond Lengths (Å) and Angles (°) for **3**

Cu1–N1	1.919(2)	Cu1–O2	1.934(2)
Cu1–N2	2.024(2)	Cu1–O5	2.050(2)
Cu1–O4	2.429(2)	Cu2–N3	1.931(2)
Cu2–N4	2.030(2)	Cu2–O8	1.951(2)
Cu2–O6	2.055(2)	Cu2–O7	2.345(2)
N2–Cu1–O2	160.41(9)	N2–Cu1–N1	82.36(9)
O2–Cu1–N1	100.87(9)	N2–Cu1–O5	82.49(8)
O2–Cu1–O5	94.02(8)	N1–Cu1–O5	164.74(9)
N2–Cu1–O4	115.96(9)	O2–Cu1–O4	83.56(9)
N1–Cu1–O4	88.00(10)	O5–Cu1–O4	97.01(8)
N3–Cu2–O8	167.10(9)	N3–Cu2–N4	83.51(9)
N4–Cu2–O8	100.96(9)	N3–Cu2–O6	82.04(8)
O8–Cu2–O6	92.97(7)	O6–Cu2–N4	165.52(9)
N3–Cu2–O7	106.82(9)	O8–Cu2–O7	89.68(8)

and **3**, respectively.

Results and Discussion

Comments on the Syntheses and Crystal Structures. Complexes **1**–**3** were synthesized according to the pathways shown in Scheme 2. The dicopper(II) units $[Cu_2(trans\text{-}L)]^{2+}$ (L = oxen or oxap) were formed when an equivalent amount $Cu(ClO_4)_2 \cdot 6H_2O$ was added to the aqueous solution of $CuL \cdot nH_2O$ (L = oxen, $n = 2$; L = oxap, $n = 0$). The aqueous solution (pH = 6–7) containing equivalent amounts of Hnic and NaOH (dissociation constant pK for Hnic is 4.82) was then added to the solution of the dicopper(II) units. Complex **1** was obtained if the molar ratio $[Cu_2(trans\text{-}L)]^{2+}$:nic was 1:1, whereas the molar ratio of 1:2 gave complex **2**. When the aqueous solution (pH = 6–7) of Hhyba and an equivalent amounts of NaOH was added to the solution of the dicopper unit ($[Cu_2(trans\text{-oxen})]^{2+}$:hyba = 1:1), a small amount of blue precipitation appeared and was filtrated. Crystals of **3** grew from the filtrate. As the aqueous solution (pH = 9–10) of Hhyba and two equivalent amounts of NaOH was added to the dicopper unit ($[Cu_2(trans\text{-oxen})]^{2+}$:hyba = 1:1), a large amount of the blue precipitation appeared, but the filtrate is colorless and no product was obtained (dissociation constants for Hhyba are $pK_1 = 4.58$ and $pK_2 = 9.23$). In this case, the dinuclear unit dissociates to form the precipitate $Cu(OH)_2$.[10]

$[\{Cu_2(trans\text{-oxap})(nic)(H_2O)_2\}_n]$ $(ClO_4)_n \cdot 0.5nH_2O$ 1: This complex contains the cationic chain, the perchlorate ions and solvated water molecules (Fig. 1). The chain is formed by the building blocks $[Cu_2(trans\text{-oxap})]^{2+}$ bridged by nic utilizing the pyridyl nitrogen and one of the carboxyl oxygen atoms to ligate the copper(II) ions in an asymmetric end-to-end mode. The intrachain Cu···Cu distance across the oxap bridge is 5.227 Å, whereas that across the spacer nic is 8.274 Å. One type of dinuclear unit contains Cu(1), whose square-based pyramidal coordination geometry is completed by the pyridyl N5 of nic equatorially and O1w axially. The other type of dinuclear unit contains Cu(2), whose coordination geometry is completed by the carboxyl oxygen O(3) of nic equatorially

Table 3. Selected Bond Distances (Å) and Angles (°) for **2**

Cu1–N1	1.9285(12)	Cu1–N5	1.9913(12)
Cu1–O1	2.0209(10)	Cu1–N2	2.0643(12)
Cu1–O8w	2.2556(10)	Cu2–N3	1.9262(12)
Cu2–N6	1.9940(12)	Cu2–O2	2.0143(10)
Cu2–N4	2.0478(12)	Cu2–O7w	2.3542(11)
N1–Cu1–N5	169.92(5)	N1–Cu1–O1	82.73(4)
N5–Cu1–O1	92.59(4)	N1–Cu1–N2	82.01(5)
N5–Cu1–N2	100.40(5)	O1–Cu1–N2	160.21(4)
N1–Cu1–O8w	97.76(4)	N5–Cu1–O8w	91.75(4)
O1–Cu1–O8w	98.69(4)	N2–Cu1–O8w	95.79(4)
N3–Cu2–N6	166.50(5)	N3–Cu2–O2	83.15(4)
N6–Cu2–O2	93.60(4)	N3–Cu2–N4	81.60(5)
N6–Cu2–N4	100.21(5)	N4–Cu2–O2	164.09(4)
N3–Cu2–O7w	103.73(4)	N6–Cu2–O7w	89.53(4)
O2–Cu2–O7w	93.81(4)	N4–Cu2–O7w	94.16(4)

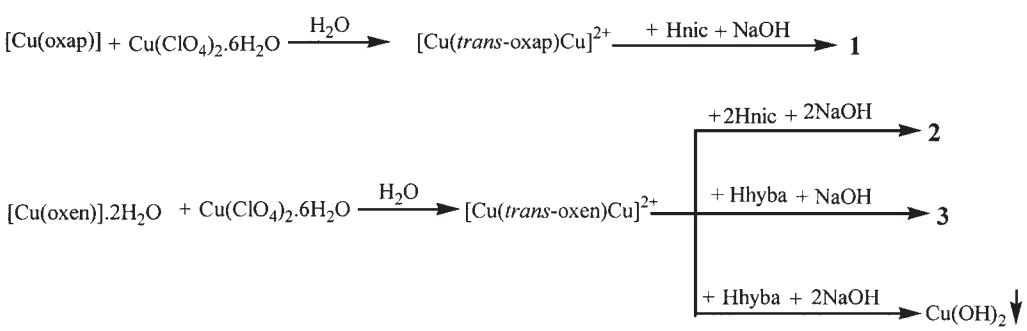

Scheme 2.

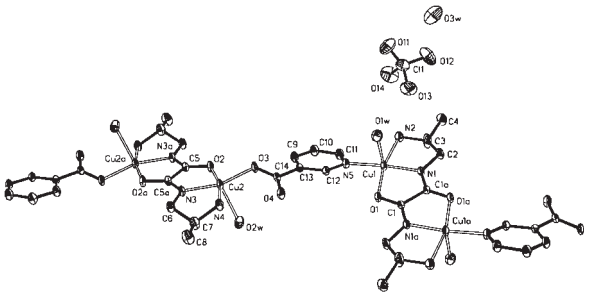

Fig. 1. ORTEP structure with atomic labeling of [{Cu_2-(*trans*-oxap)(nic)$(H_2O)_2$}$_n$]$(ClO_4)_n \cdot 0.5nH_2O$ **1**, atoms are drawn with 30% probability ellipsoids. Hydrogen atoms were omitted for clarity.

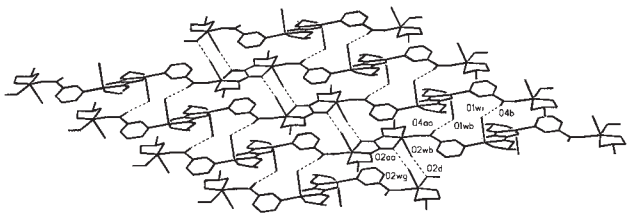

Fig. 2. Packing view of the cationic chains [Cu_2(*trans*-oxap)(nic)$(H_2O)_2]_n^{2+}$ of **1** connecting through the hydrogen bond interactions between the coordinated solvated water molecules, the amido groups, and the carboxylate groups.

and O2w axially. Each oxap ligand is a mesomer containing two asymmetric carbon atoms with opposite handedness.

Hydrogen bonds form between the ligated water molecule, the uncoordinated carboxyl oxygen and the amido oxygen of oxap. The puckered 2-D structure in Fig. 2 is derived from chains joined through two hydrogen-bonding pathways: one between the amido oxygen and the coordinated water (O2wb···O2d 2.803 Å), the other between the non-coordinated carboxyl oxygen and the coordinated water (O1wb···O4aa 2.848 Å). The ClO_4^- ions, associated with the polymeric chain through hydrogen bonds O1w···O13c (2.917 Å) and O3wa···O13 (2.843 Å), are located in the gaps between the layers (Table 5).

[Cu_2(*trans*-oxen)(nic)$_2$$(H_2O)_2$]·2$H_2O$ 2: This complex contains the discrete dinuclear unit [Cu_2(*trans*-oxen)(nic)$_2$-$(H_2O)_2$] and the solvated water molecules (Fig. 3). The square-based pyramidal geometry of Cu(II) is completed by the pyridyl nitrogen (N5 for Cu(1), N6 for Cu(2)) of nic equatorially and by H_2O (O7w for Cu(2), O8w for Cu(1)) axially. The ligand nic coordinates to Cu(II) only through the pyridyl nitrogen, while the carboxyl group is free from coordination and participates only in intermolecular hydrogen-bonding interactions.

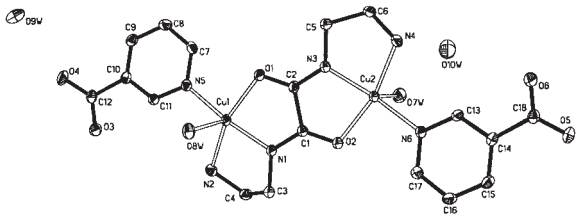

Fig. 3. ORTEP structure with atomic labeling of [Cu_2-(*trans*-oxen)(nic)$_2$$(H_2O)_2$]·2$H_2O$ **2**, atoms are drawn with 30% probability ellipsoids. Hydrogen atoms were omitted for clarity.

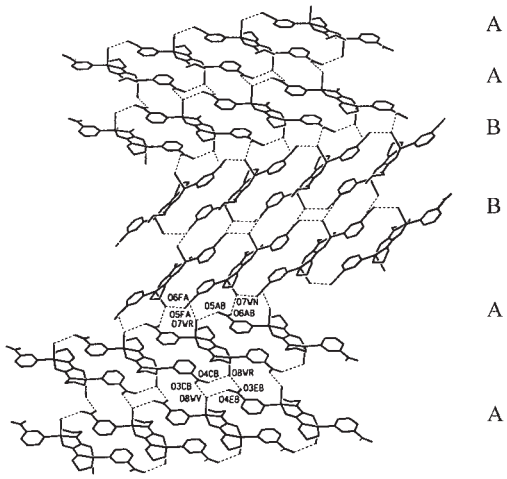

Fig. 4. Packing view of the 2-D layer of **2** constructed via hydrogen bond interactions by the chains formed through the π–π interactions between the dinuclear units.

The supramolecular architecture of **2** is interesting: it is composed of two types of chains, A and B, as shown in Fig. 4 in the sequence of AABBAABB.... All chains are formed by the dinuclear units through the intermolecular π–π stacking between the pyridyl rings, which are further connected by hydrogen bonds between the coordinated water molecules and carboxyl groups to form the layer structure. The orientation of chain A and chain B is anti-parallel (Fig. 4). The hydrogen bond pathways across chains A and B are between O7w and the car-

Table 5. Hydrogen Bond Distances (Å) for **1**, **2**, and **3**

Complex	Bond	Distance	Bond	Distance
1	O2wb···O2d	2.803	O1wb···O4aa	2.848
	O1w···O13c	2.917	O3wa···O13	2.843
2	O7wn···O6ab	2.772	O7wr···O5ab	2.795
	O8wv···O3cb	2.742	O8wv···O4eb	2.828
	O9w···O4	2.830	O9w···O3	2.742
	O10w···O5	2.799	O10w···O6	2.772
3	O4a···O5	3.011	O7···O6c	2.842
	O1···O4b	2.974	O1···O9a	2.672
	O10c···O3	2.619		

boxyl oxygen atoms O6 and O5 (O7wn···O6ab 2.772 Å, O7wr···O5ab 2.795 Å). The other types of pathway across chains A and A (or B and B) are carboxyl oxygen atoms between O8w, O3, and O4 (O8wv···O3cb 2.742 Å, O8wv···O4eb 2.828 Å). Furthermore, hydrogen bonds between solvated water molecules (O9w, O10w) and carboxyl oxygen atoms (O3, O4, O5 and O6) connect the neighboring layers to generate the 3-D supramolecular network (O9w···O4 2.830 Å, O9w···O3 2.742 Å, O10w···O5 2.799 Å, O10w···O6 2.772 Å). Consequently, each atom in the hydrogen bond system participates in the formation of two hydrogen bonds.

[Cu_2(*trans*-oxen)(hyba)$_2$(H_2O)$_2$] 3: As shown in Fig. 5, the square-based pyramidal Cu(II) is ligated by one carboxyl oxygen of hyba equatorially and by H_2O axially. The ligand hyba coordinates to copper(II) through one oxygen of the carboxyl group. The hydroxyl group is free from coordination and participates in hydrogen bond formation only.

The dinuclear units [(*trans*-oxen)(hyba)$_2$(H_2O)$_2$] are connected through three types of hydrogen bond linkages, as shown in Fig. 6. One occurs between the coordinated H_2O (O4, O7) and the amido oxygen (O5, O6) (O4a···O5 3.011 Å, O7···O6c 2.842 Å), the second between the coordinated H_2O and the hydroxyl O1 (O1···O4b 2.974 Å), and the third between the hydroxyl group (O1 or O10) and the carboxyl oxygen (O3 or O9) (O1···O9a 2.672 Å, O10c···O3 2.619 Å). The 3-D network of **3** constructed by the dinuclear units through hydrogen bonds is displayed in Fig. 7.

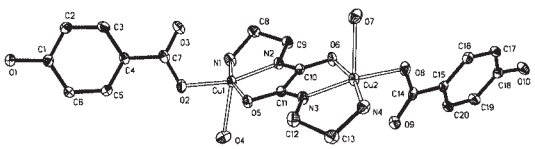

Fig. 5. ORTEP structure with atomic labeling of [Cu_2-(*trans*-oxen)(hyba)$_2$(H_2O)$_2$] **3**, atoms are drawn with 30% probability ellipsoids. Hydrogen atoms were omitted for clarity.

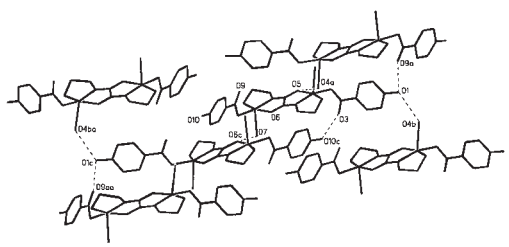

Fig. 6. The intermolecular hydrogen bond interactions in [Cu_2(*trans*-oxen)(hyba)$_2$(H_2O)$_2$] **3**.

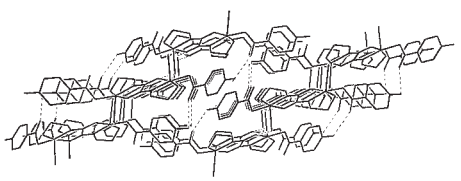

Fig. 7. Packing view of [Cu_2(*trans*-oxen)(hyba)$_2$(H_2O)$_2$] **3** showing the 3-D network.

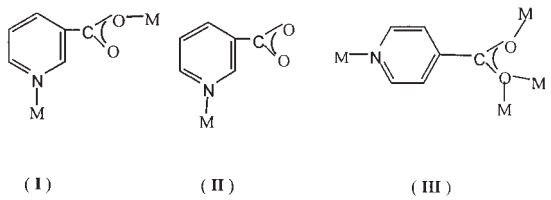

(I) (II) (III)

Chart 1.

Why are these three structures different? The affinity order of coordination groups in nic and hyba for the copper(II) is pyridyl N > COO^- > OH.[10a,11] Since the pyridyl nitrogen of nic is more prone to coordinate the copper(II) ion than the carboxyl group, when the molar ratio [Cu_2(*trans*-L)]$^{2+}$:nic was 1:2, the pyridyl moieties firstly coordinate the copper(II) and the complex [Cu_2(*trans*-oxen)(nic)$_2$(H_2O)$_2$]·2H_2O **2** with two nic was obtained. As the molar ratio of [Cu_2(*trans*-L)]$^{2+}$:nic was 1:1, the amount of nic is insufficient to coordinate the Cu(II) ions and the remaining sites of the copper(II) are filled by the carboxyl group to give [{Cu_2(*trans*-oxap)(nic)-(H_2O)$_2$}$_n$](ClO_4)$_n$·0.5*n*H_2O **1** with one nic. In the case of hyba, though the molar ratio of [Cu_2(*trans*-oxen)]$^{2+}$:hyba was 1:1, the complex [Cu_2(*trans*-oxen)(hyba)$_2$(H_2O)$_2$] **3** with two hyba was obtained since the deprotonated carboxylate group is a better donor than OH. The effort to obtain a complex containing the deprotonate OH as the spacer connecting the dinuclear copper(II) units failed.

As described above, nic in **1** acts as a spacer exhibiting the bis-monodentate character κ^1-*N*, κ^1-*O* by coordinating one copper center through the nitrogen atom and another through the carboxylate oxygen atom in an asymmetric end-to-end mode (**I**) (Chart 1), while it acts as a monodentate κ^1-*N* ligand (**II**) in **2** by coordinating the copper through the pyridyl nitrogen atom only. Consequently, 1-D polymer is formed in **1** and the discrete complex in **2**. The free carboxylate group in **2** and the OH in **3**, which are both good donors and acceptors for hydrogen bonds,[12] participate in the formation of a series of hydrogen bonds linking the discrete dinuclear complexes into extended systems. Though the group –NH_2 is a good candidate for hydrogen bond interactions, it participates in formation of hydrogen bonds that are much weaker than those mentioned above in these three complexes. In the previously reported complex [{Cu_2(*trans*-oxen)(pyca)(H_2O)}$_n$](ClO_4)$_n$·2*n*H_2O[13] (Hpyca = pyridine-4-carboxylic acid), the spacer pyca adopts the coordination mode κ^1-*N*, κ^1-*O*, μ_2-*O* bridging four copper atoms (**III**). This may be related to the different orientations of coordinating donors in pyca and nic.

In summary, extended networks constructed by the *trans*-oxamidato-bridged dicopper building blocks can be assigned to two types: in one, the coordination polymers are formed through metal–ligand interactions and supramolecular assemblies with higher dimensionality are constructed through hydrogen-bonding interactions. In the other, the extended networks were constructed directly by binuclear complex units through intermolecular interactions. A discrete binuclear complex without extended network has been reported if the spacer does not participate in intermolecular interactions,[14] indicating that the selection of suitable auxiliary ligands is a critical strategy in the fabrication of supramolecular architectures.

Table 6. TGA Data of **1**, **2**, and **3**

Complex	Dehydration temperature range/°C	Wt loss (measured) /%	Wt loss (calcd) /%	Number of water molecules lost	Decomposition temp/°C
1	100–140	11.9	14.0	4	250
2	90–137	15.6	14.8	4	247
3	120–140	7.8	7.5	2.5	282

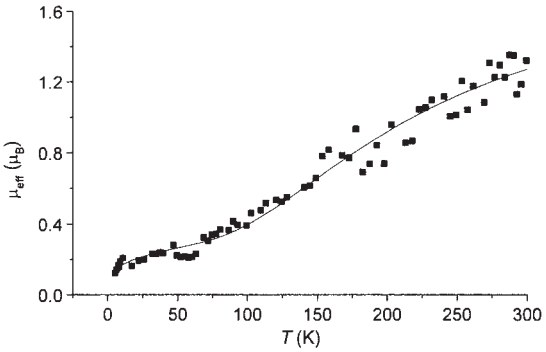

Fig. 8. A plot of the temperature dependence of the effective magnetic moments μ_{eff} for $[Cu_2(trans\text{-oxen})(hyba)_2(H_2O)_2]$ **3**. The solid line represents the theoretical calculated curve. The dots (■) represent the experimental data.

Magnetism, Infrared Spectra, and TGA. The temperature dependence of the effective magnetic moment per molecule of **3** in the form of μ_{eff} vs T is shown by the dots in Fig. 8. The fact that the effective magnetic moment (μ_{eff}) decreases gradually with the decrease of temperature reveals an antiferromagnetic interaction in this complex. Two kinds of magnetic pathways can be considered in **3**. One is through the intramolecular oxen ligand and the other is through intermolecular hydrogen bonds. Oxamidate ligands are known to have a remarkable efficiency to propagate antiferromagnetic coupling between copper(II) ions when the sets of oxygen and nitrogen donors occupy equatorial sites in the metal surroundings.[9b,15] The magnetic orbitals in **3** point from the copper(II) towards the four equatorial donors and overlap either side of the bridge oxen; strong antiferromagnetic interactions can thus be expected within the dinuclear unit. A very small spin density is in the apical position of each copper(II), so the magnetic coupling through hydrogen bonds is expected to be small due to the orientations of hydrogen bonds in apical positions and the large distances between intermolecular Cu(II) ions. Therefore, so the magnetic coupling system of **3** can be considered as interacting dimeric units $[Cu(trans\text{-oxen})Cu]^{2+}$ with coupling constant J, while that through hydrogen bond interactions creates an inter-dimeric molecular field (θ). On this basis, it should be possible to interpret the data by means of a modified Bleaney–Bowers equation[16] with an intermolecular interaction:

$$\chi_M = \frac{2N\beta^2g^2}{k(T-\theta)}\left[3+\exp\left(-\frac{J}{kT}\right)\right]^{-1}(1-\rho) + \frac{N\beta^2g^2}{2k(T-\theta)}\rho + 2N_\alpha, \quad (1)$$

$$\mu_{eff}(Cu) = 2.828\sqrt{\chi_M T/2}. \quad (2)$$

Least-squares fitting of the experimental data led to $J = -391.40$ cm^{-1}, $g = 2.08$, $\theta = -7.40$ K, and $\rho = 0.01$, where ρ is the percentage of the paramagnetic impurities, N_α is the temperature-independent paramagnetism. The symbols N, β and k have their usual meanings. The curve calculation with these parameters gave a reasonably satisfactory fit to the experimental data as shown by the solid line in Fig. 8. The strong antiferromagnetic interaction in **3** is in agreement with that reported for other oxen-bridged copper(II) complexes: values of -335 and -516.8 cm^{-1} were reported for the complexes $[Cu_2(oxen)(4,4'\text{-bipy})_2]_n\cdot[ClO_4]_{2n}$[5d] and $[Cu_4(oxen)_2(N_3)_3]_n\cdot[ClO_4]_n\cdot 2nH_2O$.[5c] The negative θ reveals that the total contribution for hydrogen bonds is antiferromagnetic.

In the IR spectra, the absorption bands in the regions 1540–1600 and 1350–1400 cm^{-1} correspond to the asymmetric and symmetric vibrations of the carboxylate moiety, respectively. Compared to the corresponding Δ value [$\Delta = \nu_{as}(COO^-) - \nu_s(COO^-)$] of Nanic (205 cm^{-1}), the Δ values of **1** (225 cm^{-1}) and **2** (204 cm^{-1}) indicate that nic in **1** coordinates the copper(II) ions in a monodentate fashion and nic in **2** is uncoordinated. The absorption of 1103 and 620 cm^{-1} indicates that ClO_4^- is a free anion. The Δ value (195 cm^{-1}) of **3** indicates that the carboxylate group coordinates the copper(II) ion in a monodentate fashion.

The TGA results (Table 6) showed that three complexes lost the water molecules between 100 and 140 °C. After the dehydration, complexes are stable up to the temperature 230–285 °C.

Conclusion

In this paper, the combination of oxamidato and nic or hyba provide rich oxygen and proton sites for hydrogen bonds and aromatic rings for π–π stacking; thus it is easy to construct supramolecular networks. Suitable selection of spacers and substituents on oxamide could allow us to fabricate more new structures "by-design", when we have learnt better the regularities of structural directional traits of these ligands.

This work was supported by the NNSF of China, the NSF of Guangdong Province, and the Starting Research Fund for Young Teachers of ZSU.

References

1 a) J.-M. Lehn, "Supramolecular Chemistry," VCH, New York (1995). b) F. Vögtle, "Supramolecular Chemistry," Wiley, Chichester (1991). c) G. R. Desiraju, *Chem. Commun.*, **1997**, 1475.

2 a) S. R. Batten and R. Robson, *Angew. Chem., Int. Ed.*, **38**, 1460 (1999). b) N. Takeda, K. Umemoto, K. Yamaguchi, and M. Fujita, *Nature*, **398**, 794 (1999). c) D. K. Chand, K. Biradha, M. Fujita, S. Sakamoto, and K. Yamaguchi, *Chem. Commun.*, **2002**,

2486. d) M. J. Zaworotko, *Chem. Commun.*, **2001**, 1.

3 M. Eddaoudi, D. B. Moler, H. Li, B. Chen, T. M. Reineke, M. O'Keeffe, and O. M. Yaghi, *Acc. Chem. Res.*, **34**, 319 (2001).

4 a) D. Braga, *J. Chem. Soc., Dalton Trans.*, **2000**, 3705. b) C. B. Aakeröy, A. M. Beatty, and D. S. Leinen, *Angew. Chem., Int. Ed.*, **38**, 1815 (1999).

5 a) Z. N. Chen, H. X. Zhang, C. Y. Su, Z. Y. Zhou, K. C. Zheng, and B. S. Kang, *Inorg. Chem.*, **37**, 3877 (1998). b) Z. N. Chen, H. X. Zhang, K. B. Yu, B. S. Kang, H. Cai, C. Y. Su, T. W. Wang, and Z. L. Lu, *Inorg. Chem.*, **37**, 4775 (1998). c) Z. N. Chen, J. Qiu, Z. K. Wu, D. G. Fu, K. B. Yu, and W. X. Tang, *J. Chem. Soc., Dalton Trans.*, **1994**, 1923. d) Z. N. Chen, D. G. Fu, K. B. Yu, and W. X. Tang, *J. Chem. Soc., Dalton Trans.*, **1994**, 1917.

6 H. X. Zhang, B. S. Kang, Z. Y. Zhou, A. S. C. Chan, K. B. Yu, Z. N. Chen, and C. Ren, *Inorg. Chem. Commun.*, **4**, 695 (2001).

7 a) Z. N. Chen, H. X. Zhang, K. B. Yu, and B. S. Kang, *Chem. Lett.*, **1998**, 275. b) Z. N. Chen, H. X. Zhang, K. B. Yu, K. C. Zheng, H. Cai, and B. S. Kang, *J. Chem. Soc., Dalton Trans.*, **1998**, 1133.

8 a) H. X. Zhang, B. S. Kang, A. W. Xu, Z. N. Chen, and H. Q. Liu, *Comments Inorg. Chem.*, **23**, 231 (2002). b) H. X. Zhang, B. S. Kang, Z. Y. Zhou, A. S. C. Chan, Z. N. Chen, and C. Ren, *J. Chem. Soc., Dalton Trans.*, **2001**, 1664. c) H. X. Zhang, B. S. Kang, A. W. Xu, Z. N. Chen, Z. Y. Zhou, A. S. C. Chan, K. B. Yu, and C. Ren, *J. Chem. Soc., Dalton Trans.*, **2001**, 2559.

9 a) J. A. Real, R. Ruiz, J. Faus, F. Lloret, M. Julve, Y. Journaux, M. Philoche-Levisalles, and C. Bios, *J. Chem. Soc., Dalton Trans.*, **1994**, 3769. b) A. Bencini, C. Benelli, A. C. Fabretti, G. Franchini, and D. Gatteschi, *Inorg. Chem.*, **25**, 1063 (1986). c) A. Cornia, A. C. Fabretti, F. Ferraro, D. Gatteschi, and A. Giusti, *J. Chem. Soc., Dalton Trans.*, **1993**, 3363.

10 a) F. Lloret, M. Julve, J. Faus, R. Ruiz, I. Castro, M. Mollar, and M. Philoche-Levisalles, *Inorg. Chem.*, **31**, 784 (1992). b) R. Ruiz, J. Faus, F. Lloret, M. Julve, and Y. Journaux, *Coord. Chem. Rev.*, **193–194**, 1069 (1999).

11 F. Lloret, M. Julve, J. Faus, Y. Journaux, M. Philoche-Levisalles, and Y. Jeannin, *Inorg. Chem.*, **28**, 3702 (1989).

12 C. B. Aakeröy, G. S. Bahra, P. B. Hitchcock, Y. Patell, and K. R. Seddon, *J. Chem. Soc., Chem. Commun.*, **1993**, 152.

13 Z. N. Chen, S. X. Liu, J. Qiu, Z. M. Wang, J. L. Huang, and W. X. Tang, *J. Chem. Soc., Dalton Trans.*, **1994**, 2989.

14 H. X. Zhang, Z. N. Chen, K. B. Yu, and B. S. Kang, *Inorg. Chem. Commun.*, **2**, 223 (1999).

15 Y. Journaux, J. Sletten, and O. Kahn, *Inorg. Chem.*, **25**, 439 (1986).

16 K. S. Suslick and C. T. Chen, *Polym. Mater. Sci. Eng.*, **63**, 272 (1990).

17 H. Ojima and K. Yamada, *Nippon Kagaku Zasshi*, **89**, 490 (1968).

18 G. M. Sheldrick, SHELXTL-PC, Siemens Analytical X-ray Instruments, Inc., Madison, WI (1990).

19 SHELXTL PC, SHELXTL 5.1, Bruker AXS Inc., Madison, WI (1998).